



Fundamental properties of bulk water from cluster ion data

JAMES V. COE†

Department of Chemistry, Ohio State University, 100 W. 18th Avenue,
Columbus, OH 43210-1173, USA

Several collaborative efforts involving the Coe group are described that connect the properties of aqueous clusters to bulk. Success in connecting cluster properties to bulk has led to new insights and reassessed properties of bulk water including, firstly, the determination of the absolute bulk hydration enthalpy and free energy of the proton using experimental clustering data on $A^\pm(H_2O)_n$ ions and, secondly, the determination of the bandgap V_0 and a new energy diagram for bulk water using experimental detachment and dissociation spectra of $(H_2O)_n^-$ hydrated electron species. The results should be of interest to anyone studying ions in water.

Contents

1. Introduction	34
2. Absolute hydration enthalpy and free energy of the proton	34
2.1. Typical absolute proton hydration enthalpies	34
2.2. Applying ion clusters to the problem	35
2.3. Equations relating cluster data to the proton's absolute hydration enthalpy	36
2.4. The need to reassess the proton's value: $n^{-4/3}$ extrapolation	38
2.5. The cluster-pair-based common-point method	38
2.6. A role for <i>ab initio</i> work	40
2.7. Predicting absolute hydration enthalpies and free energies of other ions	41
2.8. The proton's absolute solvation enthalpy in ammonia	42
2.9. Cluster ion solvation energetics over the whole cluster size range	43
3. Hydrated electron cluster data and bulk water's bandgap and energy diagram	44
3.1. Fitting to the Gaussian–Lorentzian empirical form	44
3.2. Extrapolation of full photoelectron spectrum to the bulk	47
3.3. Surface versus internal issue in hydrated electron clusters	48
3.4. Threshold issues in water	50
3.5. V_0 or the liquid electron affinity of water	50
3.6. The anion problem and the adiabatic bandgap of water	52
3.7. The chemical identity and value of the adiabatic bandgap of water	53
3.8. New bulk energy diagram of water	54
4. Conclusions	56
References	57

† Email: coe.1@osu.edu

1. Introduction

In order to make estimates of the energy changes of reactions of oppositely charged cluster ions (Plastringe *et al.* 1995, Cohen *et al.* 1996) over the whole size range, we became interested in characterizing the energetics of both $A^\pm(H_2O)_n$ ions and $(H_2O)_n$ over the whole cluster size range. Each cluster topic where we have endeavoured to make the connection to bulk has involved surprises, that is reassessments of fundamental aqueous properties. Cluster studies aimed at connecting to bulk usually begin with knowledge of monomeric gas-phase molecules, maybe dimers and small clusters, as well as bulk properties; so the work consists of characterizing the properties of intermediate-size clusters which may have energetics and structure different from both the gas phase and the bulk. In this sense, clusters represent one of the last frontiers of materials science. The current studies are somewhat different and surprising in that the bulk properties of water are being reassessed, which is unexpected for such a fundamentally important material. Since cluster properties must grow into bulk properties as clusters become large, extrapolations from sufficiently large clusters must be consistent with bulk properties. Clusters therefore offer new constraints and a different perspective on bulk which can be effectively applied to bulk properties with historic difficulties as addressed in this review. The cluster approach is first applied to the problem of the absolute hydration enthalpy of the proton and then to the role of the electron in the bulk energy diagram of water as constrained by extrapolating hydrated electron cluster studies. The latter activity has led to major reassessments of the bandgap and liquid electron affinity of water and a new energy diagram of bulk water. The results described within should be of particular interest to anyone studying ions in water.

2. Absolute hydration enthalpy and free energy of the proton

2.1. Typical absolute proton hydration enthalpies

A time line of different values for the absolute hydration enthalpy of the proton ($H^+(g) \rightarrow H^+(aq)$) has been provided by Grunwald and Steel (1996). This is the kind of property that one would expect to find in physical chemistry textbooks; however, few tackle the topic, indicating difficulties. A value of $-1090 \text{ kJ mol}^{-1}$ is given in Atkins' text (1994, p. 88†). Traditional values scatter in the vicinity of $-1100 \text{ kJ mol}^{-1}$ (Friedman and Krishnan 1973, Marcus 1994). A value of $-1103 \pm 7 \text{ kJ mol}^{-1}$ has been obtained by assuming that various tetraphenyl ions have the same volume (Marcus 1987) (TATB extra thermodynamic assumption). Sets of single-ion values often give a proton value, such as $-1129 \text{ kJ mol}^{-1}$ from that of Friedman and Krishnan (1973) based on calculated entropies; however, it is more informative to consider this in terms of an uncertainty obtained by adding the values of oppositely charged pairs of ions in the set for comparison to known experimental sums (Tissandier *et al.* 1998, table 1). The value obtained by Friedman and Krishnan becomes $-1129 \pm 32 \text{ kJ mol}^{-1}$, which has an unacceptably large uncertainty for a quantity that will be cycled into so many other quantities. Randles (1956) determined a set of absolute single-ion hydration enthalpies from electrochemical 'separation' measurements. Using well known experimental bulk ion differences (Tissandier *et al.* 1998, table 2), each single-ion value can be turned into a value for the proton. The average

† Without reference, perhaps from Halliwell and Nyberg (1963).

Table 1. Fitted slopes m_n and intercepts b_n of $\Delta H_{\text{aq}}^{0,\text{abs}}[\text{H}^+]_{\text{approx}}$ and $\Delta G_{\text{aq}}^{0,\text{abs}}[\text{H}^+]_{\text{approx}}$ versus $-\frac{1}{2}[k(\text{A}^+) + k(\text{B}^-)]$

Cluster size n	Enthalpy slope	Enthalpy intercept (kJ mol ⁻¹)	Free-energy slope	Free-energy intercept (kJ mol ⁻¹)
0	1.0000	0.0	1.0000	0.0
1	0.6956	-349.1	0.6678	-366.0
2	0.5088	-565.6	0.4535	-602.9
3	0.3762	-718.0	0.3180	-753.5
4	0.2871	-819.5	0.2430	-836.4
5	0.2137	-901.6	0.1987	-884.8
6	0.2200	-900.0	0.1514	-935.0

Table 2. Experimental and calculated stepwise clustering enthalpy for $\text{Z} + \text{H}_2\text{O} \rightarrow \text{Z}(\text{H}_2\text{O})$.

Z	$\Delta H_{0,1}$ (kJ mol ⁻¹)		
	Hybrid DFT B3LYP/ 6-311 + + G**	<i>Ab initio</i> MP2/aug- cc-pVDZ or MP2/CBS	Experimental
Li ⁺	-145	-143	(-142)
Na ⁺	-101	-97.5	-100, -111
K ⁺	-71.5	-72.4	-74.9, -70.7, -81.1
Rb ⁺		-61.5	-66.5, -66.9
OH ⁻	-126		-94.1, -105, -144, -92.5, -113
F ⁻	-118	-112	(-97.5 old), -110 ^a
Cl ⁻	-56.4	-60.2	-54.8, -62.3, -61.5, (-60.2), -61.9
Br ⁻	-48.1		-52.7, -61.9

^a From Weis *et al.* (1999).

of these is -1131 ± 12 kJ mol⁻¹; however, this approach does not take into account the surface potential of water (Trasatti 1979) which might be about 13 kJ mol⁻¹. As more powerful theoretical treatments on the nature of the proton in water become available (Marx *et al.* 1999), one can expect more theoretical treatments on energetics as in the work of Tawa *et al.* (1998), which favours more negative values in the range from the literature. The values determined from cluster ion data are significantly more negative than traditional values, which is important as this quantity cycles into so many others of wide general interest.

2.2. Applying ion clusters to the problem

Early observations from Kebarle (1974), Keesee and Castleman (1980), Keesee *et al.* (1980) and Lee *et al.* (1980) noted a remarkable tendency in the stepwise clustering energetics of different ions to converge to a common functional dependence. They suggested a connection between gas-phase cluster ion hydration data and bulk single-ion hydration enthalpies. Given the well known sums of single-ion hydration enthalpies for oppositely charged pairs of ions, Klots (1981) noted that the difference in bulk hydration enthalpy of the same pair of ions was given by the sum to infinity of the stepwise clustering enthalpy differences of the pair of ions. Unfortunately, the experimental data set rarely extends very far and Klots only had a common set of

cluster data up to $n = 5$. He apparently realized that, given the common functional dependence of stepwise enthalpies, the cluster data might be largely cancelling from $n = 6$ to infinity at least over a carefully chosen set of ion pairs. Klots used the stepwise clustering data of a set of positive ions (Na^+ , K^+ , Rb^+ , Cs^+ and NH_4^+) with the data from Cl^- and Br^- together with the known bulk sums to obtain a remarkably consistent absolute proton hydration enthalpy from each ion pair averaging to $-1136 \pm 3 \text{ kJ mol}^{-1}$. (Klots' set of single-ion values has an uncertainty of $\pm 9 \text{ kJ mol}^{-1}$ when paired and compared with the experimental bulk sums of ion pairs.) It remains unstated as to why the Cl^- , Br^- , Na^+ , K^+ , Rb^+ , Cs^+ and NH_4^+ subset was chosen. One wonders why ions such as F^- , OH^- , I^- and Li^+ were left out of the scheme. Rather than having an independent determination of the proton's absolute value from cluster ion data, we have the interesting observation that consideration of this subset of ion pairs gives results consistent with Randles' experimental determination which falls outside the range of traditional values, to the negative side.

Coe (1994) and Tissandier *et al.* (1998) sought and found an independent determination from the cluster ion data. Coe's (1994) first cluster approach used the fraction of bulk solvation enthalpy sums obtained by pairs of oppositely charged ions at a common cluster size to predict differences at bulk. The predicted differences mimicked the relative variations in the experimental data and were quantitatively scaled into the experimental data with a single parameter, producing an absolute proton value of $-1152.6 \pm 6.0 \text{ kJ mol}^{-1}$. The approach differed from previous cluster work because all the possible ion pairs statistically contributed to the proton value. However, the assumed linearity of scaling constituted an extra thermodynamic assumption that was unfamiliar to most readers; so Coe, Tuttle, and coworkers joined in a search for a cluster-based approach without such extra thermodynamic assumptions.

2.3. Equations relating cluster data to the proton's absolute hydration enthalpy

Before describing the most recent cluster-pair-based approach, it is necessary to develop a few equations which govern the relation of the proton's solvation enthalpy to cluster data. As noted by Klots (1981), the difference between the absolute solvation enthalpies of a positive and a negative cluster ion goes to zero as the cluster size becomes infinite. A relation of cluster differences to the proton's absolute value $\Delta H_{\text{aq}}^{0,\text{abs}}[\text{H}^+]$ is obtained from the relation noted above by substituting definitions of conventional cluster solvation enthalpies (Tissandier *et al.* 1998), giving

$$\frac{1}{2} \lim_{m \rightarrow \infty} \{ \Delta H_{\text{aq}}^{0,\text{con}}[\text{B}^-(\text{H}_2\text{O})_m] - \Delta H_{\text{aq}}^{0,\text{con}}[\text{A}^+(\text{H}_2\text{O})_m] \} - \Delta H_{\text{f}}^0[\text{H}^+(\text{g})] = \Delta H_{\text{aq}}^{0,\text{abs}}[\text{H}^+], \quad (1)$$

where conventional quantities are indicated by the superscript con, absolute quantities are indicated by the superscript abs and $\Delta H_{\text{f}}^0[\text{H}^+(\text{g})]$ is the heat of formation of $\text{H}^+(\text{g})$ which equals $1536.2 \text{ kJ mol}^{-1}$ (Weast 1985, Lias 1997). In terms of stepwise cluster quantities (Tissandier *et al.* 1998), this becomes

$$\frac{1}{2} \left[\Delta H_{\text{aq}}^{0,\text{con}}[\text{B}^-] - \Delta H_{\text{aq}}^{0,\text{con}}[\text{A}^+] + \lim_{m \rightarrow \infty} \left(\sum_{i=1}^m \Delta H_{i-1,i}^0(\text{A}^+) - \Delta H_{i-1,i}^0(\text{B}^-) \right) \right] - \Delta H_{\text{f}}^0[\text{H}^+(\text{g})] = \Delta H_{\text{aq}}^{0,\text{abs}}[\text{H}^+], \quad (2)$$

where $\Delta H_{\text{aq}}^{0,\text{con}}$ is the standard conventional solvation enthalpy (Tissandier *et al.* 1998). The typographical errors in the values of conventional free energies given in this reference should be noted; they should be $\Delta G_{\text{aq}}^{0,\text{con}} = 108.1, 134.9$ and $172.3 \text{ kJ mol}^{-1}$

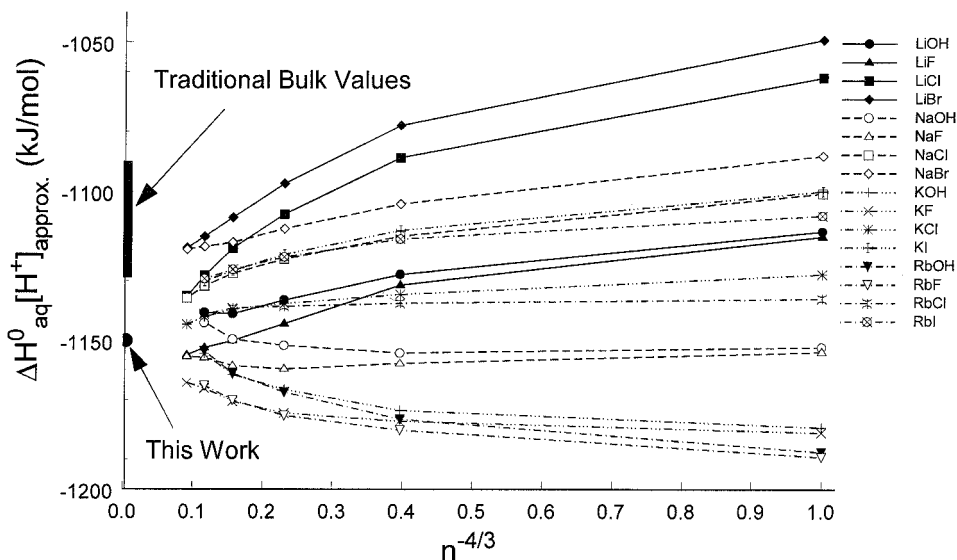


Figure 1. Motivation for a reassessment of the proton's absolute hydration enthalpy. Plot of $\Delta H_{\text{aq}}^{0,\text{abs}}[\text{H}^+]_{\text{approx}}$, the left-hand side of equation (3), versus $n^{-4/3}$, where n is the number of solvating waters about each ion in the pair. At $n = \infty$, the approximation becomes the proton's absolute hydration enthalpy exactly. The cluster data appear to be converging to a bulk value outside the traditional range of values.

for Cl^- , Br^- and I^- respectively. The $\Delta H_{i-1,i}^0$ quantities are stepwise enthalpies for adding a solvent molecule to a cluster ion of A^+ or B^- with $i-1$ solvents to make a cluster ion with i solvents (Tissandier *et al.* 1998, table 4). Note that this procedure subtracts the stepwise enthalpies for adding solvent to neutral water clusters; so such data are not needed (Klots 1981). Obviously, cluster data are not available to $m = \infty$, and it is fortunate that data up to $m = 6$ are available; so it is useful to split the stepwise sum above into a part that is known up to n (remains on the left of equation) and a part that is unknown from $n+1$ to ∞ (sent to the right), giving

$$\begin{aligned} & \frac{1}{2} \left[\Delta H_{\text{aq}}^{0,\text{con}}[\text{B}^-] - \Delta H_{\text{aq}}^{0,\text{con}}[\text{A}^+] + \left(\sum_{i=1}^n \Delta H_{i-1,i}^0(\text{A}^+) - \Delta H_{i-1,i}^0(\text{B}^-) \right) \right] - \Delta H_{\text{f}}^0[\text{H}^+(\text{g})] \\ & = \frac{1}{2} \lim_{m \rightarrow \infty} \left(\sum_{i=n+1}^m \Delta H_{i-1,i}^0(\text{A}^+) - \Delta H_{i-1,i}^0(\text{B}^-) \right) + \Delta H_{\text{aq}}^{0,\text{abs}}[\text{H}^+], \quad (3) \end{aligned}$$

The left-hand side is known, while the right-hand side is unknown. The left-hand side represents an approximation to the proton's absolute solvation enthalpy $\Delta H_{\text{aq}}^{0,\text{abs}}[\text{H}^+]_{\text{approx}}$, which becomes exact as $m \rightarrow \infty$. This equation offers concise explanations regarding the various cluster-based approaches. If conditions can be found whereby the first term on the right-hand side of equation (3) is zero, then the absolute proton solvation enthalpy is determined. This term (the sum of unknown stepwise differences for an ion pair) might average to zero for the right pairs of ions; however, it could also be that no actual pair of ions comes close enough to cancelling this term. We analyse the trends in $\Delta H_{\text{aq}}^{0,\text{abs}}[\text{H}^+]_{\text{approx}}$ to characterize the deviations of the unknown stepwise differences for real ion pairs from an ideal pair where this term would cancel. By characterizing the deviations of the whole data set, this ideal point can be determined whether or not there exists such an ideal ion pair.

2.4 The need to reassess the proton's value: $n^{-4/3}$ extrapolation

The need to reassess the proton's absolute hydration enthalpy is motivated by examining the progression of the stepwise hydration enthalpy differences of cluster ion pairs towards bulk. More specifically, the left-hand side of equation (3) is plotted versus $n^{-4/3}$ as in figure 1. This plot is similar to an $n^{-1/3}$ plot from Tissandier *et al.* (1998, figure 1). In the limit as $n \rightarrow \infty$, these data must converge to the absolute hydration enthalpy of the proton, and the data show a rapid convergence with increasing cluster size. Since ions of both polarities have solvation energetics that proceed to bulk with a common functionality (linearity in $n^{-1/3}$ at large n (Coe 1997)), the difference between a pair of oppositely charged ions will tend to cancel shared trends, producing a leading term of $n^{-4/3}$. Considering both the curvature of the trends and the linear projection of the limiting trends in $n^{-4/3}$, it is clear that the data will converge at a limiting value well outside the range of traditional values (which have been indicated in figure 1) for the proton's absolute hydration enthalpy. Malaxos *et al.* (2001) fitted the data sets for pairs of ions in figure 1 to the form

$$\Delta H_{\text{aq}}^{0,\text{abs}}[\text{H}^+]_{\text{approx}} = \alpha_0 + \alpha_1 n^{-4/3} + \alpha_2 n^{-7/3}, \quad (4)$$

where $\Delta H_{\text{aq}}^{0,\text{abs}}[\text{H}^+]_{\text{approx}}$ is the left-hand side of equation (3). The average of the bulk intercepts for each of the 20 pairs of ions shown in figure 1 gives an absolute proton value of $-1144 \pm 8 \text{ kJ mol}^{-1}$ (estimated standard deviation). This result constitutes a reasonable assessment of the experimental cluster data set's constraint upon the proton's bulk value. However, an extra thermodynamic assumption is still being made, namely that the pair differences proceed to bulk with linearity in $n^{-4/3}$.

2.5. The cluster-pair-based common-point method

While the extra thermodynamic assumption of $n^{-4/3}$ linearity in differences is one that the community may be willing to make, Malaxos *et al.* sought a method that did not make extra thermodynamic assumptions. The key to their approach can be understood by considering equation (3). If, at a particular cluster size n , one were to calculate the left-hand side of the equation for all available pairs of oppositely charged ions, then any variations would have to be due to the first term on the right-hand side because the only other term on the right-hand side is a constant, $\Delta H_{\text{aq}}^{0,\text{abs}}[\text{H}^+]$. These workers discovered that the variations in $\Delta H_{\text{aq}}^{0,\text{abs}}[\text{H}^+]_{\text{approx}}$, that is the left-hand side of equation (3), over ion pairs at a particular cluster size are linear when plotted against several possible variables, including the following:

- (i) $-\frac{1}{2}[k(\text{A}^+) + k(\text{B}^-)]$ where $k(\text{A}^+)$ and $k(\text{B}^-)$ are well known differences between the ion's (A^+ and B^-) and the proton's absolute bulk hydration enthalpies (Tissandier *et al.* 1998, table 2);
- (ii) $1/r_{\text{A}^+} - 1/r_{\text{B}^-}$, where r is the ion radius for spherical ions;
- (iii) $\Delta H_n^0(\text{A}^+) - \Delta H_n^0(\text{B}^-)$ where ΔH_n^0 is the solvation enthalpy of an ion in a water cluster of size n .

In other words, the new realization here is that

$$\begin{aligned} \frac{1}{2} \lim_{m \rightarrow \infty} \left(\sum_{i=n+1}^m \Delta H_{i-1,i}^0(\text{A}^+) - \Delta H_{i-1,i}^0(\text{B}^-) \right) &\propto -\frac{1}{2}[k(\text{A}^+) + k(\text{B}^-)] \\ &\propto \frac{1}{r_{\text{A}^+}} - \frac{1}{r_{\text{B}^-}} \\ &\propto \Delta H_n^0(\text{A}^+) - \Delta H_n^0(\text{B}^-). \end{aligned} \quad (5)$$

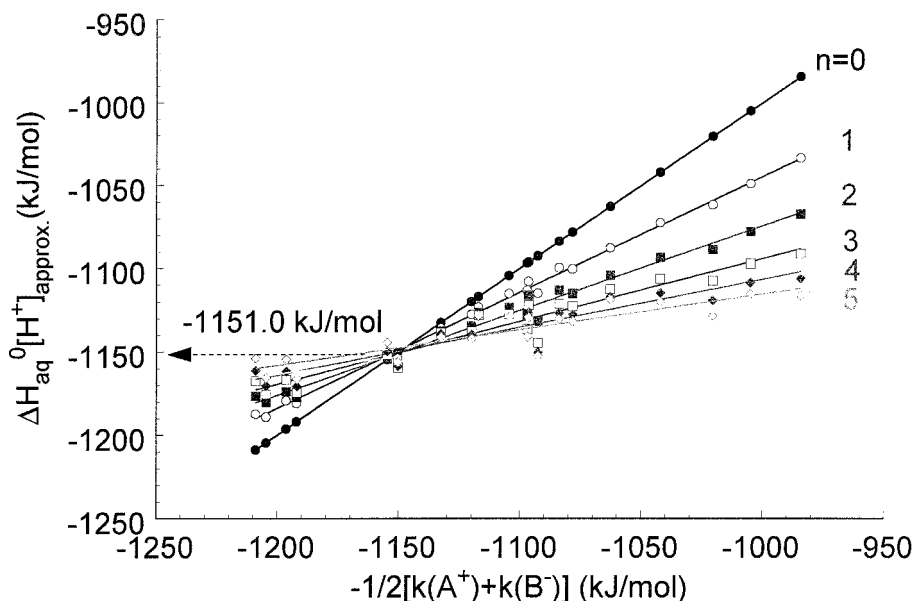


Figure 2. The cluster-pair-based common-point method for a determination of the proton's absolute hydration enthalpy without extrathermodynamic assumptions. Plot of $\Delta H_{\text{aq}}^0 [\text{H}^+]_{\text{approx}}$ versus $-\frac{1}{2}[k(\text{A}^+) + k(\text{B}^-)]$ at different cluster sizes, where $k(\text{A}^+)$ and $k(\text{B}^-)$ are well known differences between the ion's (A^+ and B^-) and the proton's absolute bulk hydration enthalpies (Tissandier *et al.* 1998, table 2). The fitted lines converge to a common point where the unknown term from equation (3), $\frac{1}{2} \lim_{m \rightarrow \infty} [\sum_{i=n+1}^m \Delta H_{i-1,i}^0(\text{A}^+) - \Delta H_{i-1,i}^0(\text{B}^-)]$, must be zero. This determines an absolute proton hydration enthalpy of $-1151.0 \pm 2.2 \text{ kJ mol}^{-1}$.

Considering that the second option in equation (5) has difficulties with non-spherical molecular ions and the third option varies with cluster size (even though these relations were discovered through this option (Tissandier *et al.* 1998)), the quantity $\Delta H_{\text{aq}}^0 [\text{H}^+]_{\text{approx}}$ is preferably plotted against the first option, $-\frac{1}{2}[k(\text{A}^+) + k(\text{B}^-)]$, for $n = 0$ to 6 as in figure 2. Linearity of the variations over ion pairs in itself is not enough because it does not tell us when the $\frac{1}{2} \lim_{m \rightarrow \infty} [\sum_{i=n+1}^m \Delta H_{i-1,i}^0(\text{A}^+) - \Delta H_{i-1,i}^0(\text{B}^-)]$ term is zero, revealing the proton's absolute value. However, with increasing cluster size, the variations over ion pairs decrease and the slope of the linear relationship changes, becoming smaller as expected. Most interestingly, linear plots at different cluster sizes share a common point! Given the regularity of the trend towards bulk, these linear plots can only share such a point in common if $\frac{1}{2} \lim_{m \rightarrow \infty} [\sum_{i=n+1}^m \Delta H_{i-1,i}^0(\text{A}^+) - \Delta H_{i-1,i}^0(\text{B}^-)] = 0$. They reveal the proton's absolute value *without making any of the usual extra thermodynamic assumptions*. The data at each cluster size are fitted to a line (table 1) and the optimal proton value is obtained from the point at which the lines have minimum sum of the squares of the deviations from each other in the y-axis coordinate. A value of $-1151.0 \pm 2.2 \text{ kJ mol}^{-1}$ results for the absolute hydration enthalpy of the proton. This is in excellent agreement with the value of $-1150.1 \pm 0.9 \text{ kJ mol}^{-1}$ obtained using cluster solvation enthalpy differences (Tissandier *et al.* 1998), that is the third option in equation (5). This result is also in good agreement with the value of $-1144 \pm 8 \text{ kJ mol}^{-1}$ (estimated standard deviation) obtained from $n^{-4/3}$ extrapolation.

The cluster ion pair common-point method works equally well for free energies.

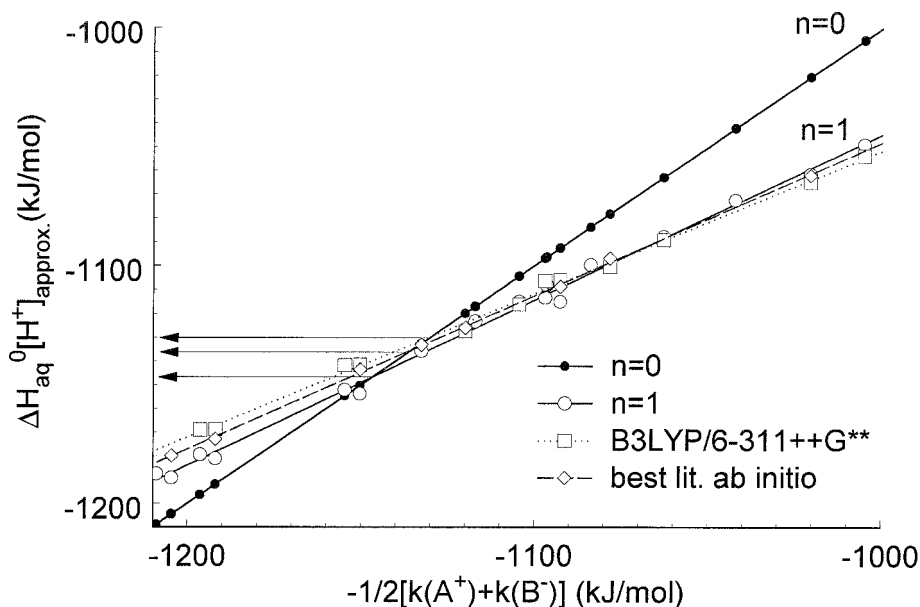


Figure 3. A plot of different methods for determining aqueous data at $n = 1$ with the cluster-pair-based common-point method: (○), experimental cluster data; (◇), the best literature *ab initio* data; (□), B3LYP/6-311++G** computed data. This exercise considers the variations obtained in the proton's absolute hydration enthalpy with a bare minimum of input for determining the common point.

One may substitute free-energy values G for the enthalpy values H in the preceding equations to have free-energy expressions. The cluster solvation free energy difference option produces a proton absolute hydration free energy of $-1104.5 \pm 0.3 \text{ kJ mol}^{-1}$ (Tissandier *et al.* 1998). Plots versus $-\frac{1}{2}[k(A^+) + k(B^-)]$ produce a proton free-energy value of $-1103.2 \pm 1.1 \text{ kJ mol}^{-1}$ (Malaxos *et al.* 2001). These results compare favourably with the centre of weight of determinations in the chronological survey of Freidman and Krishnan (1973), but to the negative side of the range of 'key' results as tabulated by Grunwald and Steel (1996). They are consistent with the recent computational results of Tawa *et al.* (1998) of $-1097 \text{ kJ mol}^{-1}$, favouring the negative side of the traditional range.

2.6. A role for *ab initio* work

An attractive feature of the new formalism when plotting $\Delta H_{\text{aq}}^{0,\text{abs}}[\text{H}^+]_{\text{approx}}$ versus $-\frac{1}{2}[k(A^+) + k(B^-)]$ is that there is an $n = 0$ line, so that cluster ion data at $n = 1$ provide a cross-over or common point. If ion clustering data are not available, such data can be accurately calculated at this size. High-level *ab initio* calculations of stepwise clustering now appear to have an accuracy similar to (if not better than) the experimental data set (Keese and Castleman 1986). In fact, a discrepancy between the old experimental $n = 1$ value for F^- and the *ab initio* result has recently been resolved (Weis *et al.* 1999) in favour of the *ab initio* result. A comparison of the experimental ion cluster data and calculated data for determining $\Delta H_{\text{aq}}^{0,\text{abs}}[\text{H}^+]$ at $n = 1$ is given in figure 3. The high-level *ab initio* data (labelled best lit. *ab initio* in figure 3) was obtained for the F^- and Cl^- anions (Xantheas 1996, Xantheas and Dang 1996) and the Li^+ , Na^+ , K^+ and Rb^+ cations (Fellers *et al.* 1995). A set of calculations (chosen to be

achievable on desk-top personal computers) was performed using the Hartree–Fock–density functional theory (DFT) hybrid method B3LYP with basis set 6-311++G** on the Li^+ , Na^+ , K^+ , OH^- , F^- , Cl^- and Br^- ions using Gaussian (Frisch *et al.* 1995). The calculations include vibrational frequencies allowing corrections for zero-point energy and thermal effects. Table 2 allows comparison of the calculated $\Delta H_{0,1}$ values for the $n = 1$ clustering reaction at 298 K with the experimental values. The calculations agree well with the experimental work which has substantial variations. The proton’s bulk values are -1147 , -1135 and -1130 kJ mol^{-1} for the experimental, best literature *ab initio* and B3LYP results respectively. This is less than 2% error in the calculated results, which may be quite acceptable for some purposes, such as in solvents where little is known about the proton’s absolute solvation enthalpy. Finally, it would be very interesting to see both the effect of taking the calculations to higher cluster size and the effect of higher levels of theory. Is there still a common point in the calculated data at larger n ? Might higher levels of theory mimic the experimental data without any systematic deviations? The literature *ab initio* anion calculations use similar but not exactly the same methods as the cations. Perhaps use of the exact same method would reduce the systematic deviations from experiment, or perhaps there are systematic errors in the experiments. Of course many of the ions in the set under consideration are fairly large; so one must balance the desire to use higher levels of theory with the desire to make calculations on all ions in the set, including Rb^+ and I^- .

2.7. Predicting absolute hydration enthalpies and free energies of other ions

The cluster-pair-based common-point method offers a potentially useful recipe for predicting bulk single-ion hydration enthalpies from small cluster data when no bulk data are available. The absolute solvation enthalpy of a general anion B^- can be related to the slopes m_n and intercepts b_n given in table 1 and an already characterized cation A^+ at a particular cluster size n as

$$\Delta H_{\text{aq}}^{0,\text{abs}}(\text{B}^-) = \Delta H_{\text{aq}}^{0,\text{con}}(\text{A}^+) - \frac{1}{1-m_n} \left(\sum_{i=1}^n \Delta H_{i-1,i}^0(\text{A}^+) - \Delta H_{i-1,i}^0(\text{B}^-) \right) + \Delta H_{\text{f}}^0[\text{H}^+(\text{g})] + \frac{2b_n}{1-m_n} - \Delta H_{\text{aq}}^{0,\text{abs}}(\text{H}^+), \quad (6)$$

where the superscripts *abs* and *con* indicate absolute and conventional values as before. As an example, let us take the O_3^- and O^- radical anions, which are important in the irradiation of alkaline oxygenated aqueous solutions (Bentley *et al.* 2000). Bentley *et al.* computed a B3LYP/6-31+G* stepwise enthalpy of $\Delta H_{0,1}(\text{O}_3^-) = -69.0$ kJ mol^{-1} for the reaction $\text{O}_3^- + \text{H}_2\text{O} \rightarrow \text{O}_3^-(\text{H}_2\text{O})$ and obtained $\Delta H_{0,1}(\text{O}^-) = -115$ kJ mol^{-1} for the reaction $\text{O}^- + \text{H}_2\text{O} \rightarrow \text{O}^-(\text{H}_2\text{O})$. When these quantities are used in equation (6) with the slope and intercept at $n = 1$ from table 1, and the set of conventional cation enthalpies from each cation from Tissandier *et al.* (1998), values of $\Delta H_{\text{aq}}^{0,\text{abs}}(\text{O}_3^-) = -345 \pm 11$ kJ mol^{-1} and $\Delta H_{\text{aq}}^{0,\text{abs}}(\text{O}^-) = -496 \pm 11$ kJ mol^{-1} are obtained for the bulk hydration enthalpies of these ions. When these results are cycled with the calculated gas-phase dissociation enthalpy of O_3^- of 169 kJ mol^{-1} (Bentley *et al.* 2000) and an estimate of 0 kJ mol^{-1} for the hydration of O_2 , one obtains an estimate of 19 kJ mol^{-1} for the dissociation enthalpy of $\text{O}_3^-(\text{aq})$. There appears to be a dramatic weakening of the $[\text{O}_2-\text{O}]^-$ bond upon solvation in water as has been pointed out in the literature (Su and Tripathi 1992, Bentley *et al.* 2000).

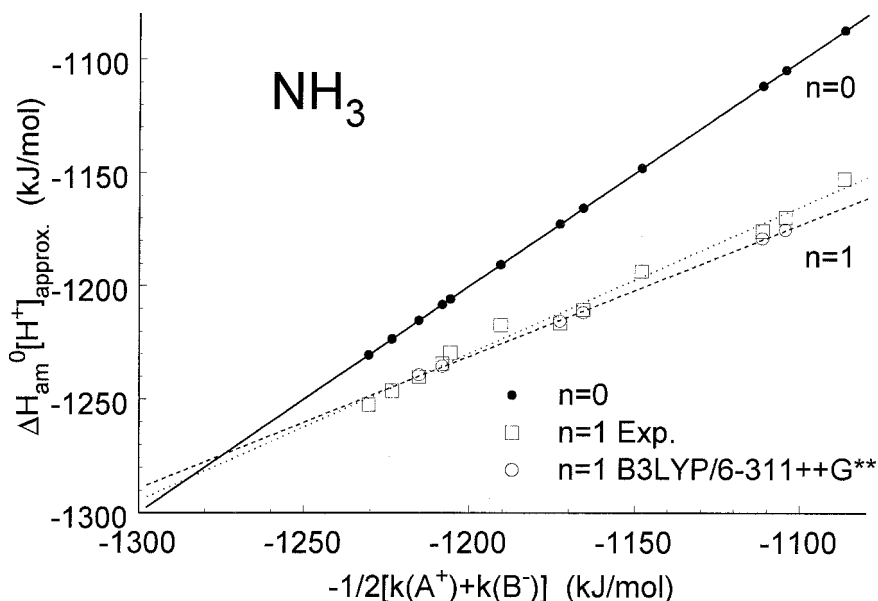


Figure 4. Plot of the cluster-pair-based common-point method in ammonia using both experimental data (\square) and B3LYP/6-311++G** computed values (\circ) at $n = 1$. Common points produce proton absolute ammoniation enthalpies of -1285 ± 16 and -1274 ± 3 kJ mol $^{-1}$ for the experimental and computed data respectively. Literature values of -1260 kJ mol $^{-1}$ (Jolly 1952, 1954) are based on the assumption that Rb $^{+}$ and Br $^{-}$ have identical bulk ammoniation enthalpies. If so, this pair would be observed at the common point. In fact, none of the ion pairs comes close to the common point.

2.8. The proton's absolute solvation enthalpy in ammonia

If the concepts of the cluster-pair based common-point method are correct, then they ought to work in other solvents. Malaxos *et al.* (2001) have begun to examine ion solvation in NH $_3$. A plot of both experimental and computed data at $n = 1$ versus $-1/2[k(A^+) + k(B^-)]$ is given in figure 4. The experimental data, including Li $^{+}$, Na $^{+}$, K $^{+}$, Rb $^{+}$, Cl $^{-}$, Br $^{-}$ and I $^{-}$, are not as extensive as in water and exhibit more scatter than the computed results (B3LYP/6-311++G**) which do not include the Rb $^{+}$ and I $^{-}$ ions. The intersection of the $n = 0$ and $n = 1$ lines lies beyond the range of the data and must be extrapolated as opposed to the case of water where these intersections can be interpolated. It is interesting that the F $^{-}$ data are insufficient to be included in the method. It would be very useful to have some experimental clustering data as well as some bulk enthalpic data on F $^{-}$. To determine the uncertainties in the intersections with the data at hand, it is necessary to carry out a full covariant propagation of the errors including the correlation between slope and intercept. With the understanding that only random errors are being characterized, the proton's absolute solvation enthalpy in ammonia is estimated to be -1285 ± 16 kJ mol $^{-1}$ from the experimental data and -1274 ± 3 kJ mol $^{-1}$ from the B3LYP/6-311++G** calculations. One should keep in mind that the intersection must be a common point (shared by the other cluster sizes) in order to be a good estimate. So, the systematic errors could be significant and have not yet been quantified. By assuming that Rb $^{+}$ and Br $^{-}$ have identical bulk ammoniation enthalpies, Jolly (1952, 1954) determined that solvation of a proton was 109 kJ mol $^{-1}$ more stable in ammonia than in water. Using our value for the proton's absolute hydration enthalpy (-1151.0 kJ mol $^{-1}$) this gives an estimate

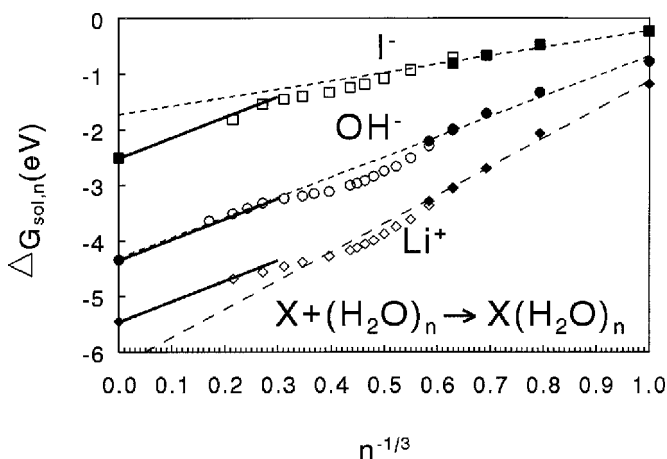


Figure 5. The hydration free energies of I^- , OH^- and Li^+ (Coe 1997) as functions of cluster size over the whole size range. The plot reveals how the hydration free energy deviates from continuum laws (—) at large cluster sizes upon entering the nanosize regime. At small cluster sizes (\blacksquare , \bullet , \blacklozenge), each ion has a unique trend determined by the strength of ion–solvent interactions that are diluted by solvent–solvent interactions in the intermediate-size range (\square , \circ , \diamond) as characterized by polar solvent simulations (Lu 1996, Lu and Singer 1996).

for the proton's absolute ammonation enthalpy of $-1260 \text{ kJ mol}^{-1}$. Schindewolf (1982) gives a value of $-1265 \text{ kJ mol}^{-1}$ in agreement with Jolly, but the 'appropriate reactions' are not explicitly given, making critical comparison difficult. Since the Rb^+ , Br^- ion pair has been used in the experimental data of figure 4, it is clear that Rb^+ and Br^- do not share a common ammonation enthalpy or they would occur at the common point. The Rb^+ , Cl^- pair is, in fact, closer to the common point than the Rb^+ , Br^- pair, and none of the ion pairs considered comes close. An absolute proton bulk ammonation value of about 20 kJ mol^{-1} more negative than previously estimated seems likely, but more work is needed, particularly on the F^- anion.

2.9. Cluster ion solvation energetics over the whole cluster size range

Given the absolute single-ion hydration values available from the cluster-pair-based common-point method (Tissandier *et al.* 1998) and the available small cluster data (Keese and Castleman 1986), it becomes interesting to consider how a property, such as an ion's solvation free energy, varies over the whole cluster size range (Coe 1997). The polar solvent simulations of Lu (1996) and Lu and Singer (1996) were found to connect the small cluster data with the similar continuum trends that large clusters must display as they proceed to bulk (Coe 1997). The data for I^- , OH^- and Li^+ (large-, same- and small-size ions relative to the solvating water molecule) are displayed in figure 5. Different ions exhibit different trends at small cluster size owing to the different strengths of ion–solvent interactions; however, all ions must go into bulk with the same limiting trend determined by the static dielectric constant of water. The intermediate-cluster-size region has a unique form arising from the dilution of ion–solvent effects by an increasing number of solvent–solvent interactions. It is important to note that the extrapolation of continuum slopes back to a small cluster size accounts rather poorly for the Li^+ and I^- data at small cluster sizes. It is only by fortuitous cancellation of small-cluster effects which vary with ion identity that the

continuum trend accounts for the OH^- small-cluster data, and it still does a poor job in the intermediate-size regime in this case. The plot in figure 5 gives us a first glimpse of the magnitude and direction of deviations in ion solvation free energy from our expectations based on bulk properties. This represents a good first step in quantifying the thermochemical properties of such nanosize particles.

3. Hydrated electron cluster data and bulk water's bandgap and energy diagram

While 12.6 eV photons are required to separate an electron from a gas-phase water molecule (Linde 1997), it only requires 6.5 eV photons to separate charge in water producing the spectrum of $e^-(\text{aq})$ (Han and Bartels 1990). What condensed states of water facilitate this large difference? As $n \rightarrow \infty$, $(\text{H}_2\text{O})_n$ clusters grow into $e^-(\text{aq})$ and can be used to characterize the regions of bulk water's energy diagram involving the electron, such as the conduction band. If we think of water as a large-bandgap amorphous semiconductor, then $e^-(\text{aq})$ can be thought of as an anionic defect state of pure water. Likewise, the tiny fraction (about 10^{-9}) of water molecules dissociated at equilibrium produce $\text{OH}^-(\text{aq})$ that can also be considered an anionic defect state of pure water. One must carefully consider the reorganization of solvating water molecules about these intrinsic anionic defect states of pure water in order to produce an energy diagram for bulk water that is consistent with the known photophysics and thermochemistry of ions in water. Such molecular details are not usually considered in the generic definitions of semiconductor properties (such as the bandgap or condensed-phase electron affinity); so there are important semantic distinctions to be made regarding the molecular nature of ion solvation, which often have not been drawn in the literature. In the following sections, hydrated electron cluster data versus cluster size on photodetachment (Coe 1986, Posey *et al.* 1989, Coe *et al.* 1990, Lee *et al.* 1991) from the Bowen group at The Johns Hopkins University and absorption spectra (Posey and Johnson 1988, Posey *et al.* 1989, Campagnola *et al.* 1991, Ayotte and Johnson 1997) from the Johnson group at Yale have been examined together (Coe *et al.* 2001) to better constrain the bulk semiconductor properties of water.

3.1. Fitting to the Gaussian–Lorentzian empirical form

Both the photoelectron (as a function of the electron binding energy) and absorption (as a function of the photon energy) cluster spectra were fitted to a well known empirical functional form (Golden and Tuttle 1981, Tuttle and Golden 1981) and were found to give good fits for the bulk absorption spectrum of $e^-(\text{aq})$. Since the quantum-mechanical expressions for photoelectron spectroscopy (fixed photon energy and measured e^- kinetic energies) are quite different from those for absorption spectroscopy (tuned photon energy and loss of photons), it is slightly surprising that the photoelectron spectra could be fitted to the same functional form. The fitting function $I(E)$ has a Gaussian form to the low-energy side of the peak and a Lorentzian form to the high-energy side, as follows:

$$\text{if } \begin{cases} E \leq E_{\max}, & I(E) = A \exp \left[-\frac{1}{2} \left(\frac{E - E_{\max}}{\sigma_G} \right)^2 \right], \\ E \geq E_{\max}, & I(E) = A \frac{1}{1 + [(E - E_{\max})/\sigma_L]^2}, \end{cases} \quad (7)$$

where E_{\max} is the energy position of the intensity maximum, σ_G is the Gaussian standard deviation characterizing the width of the low-energy side of the peak, σ_L is

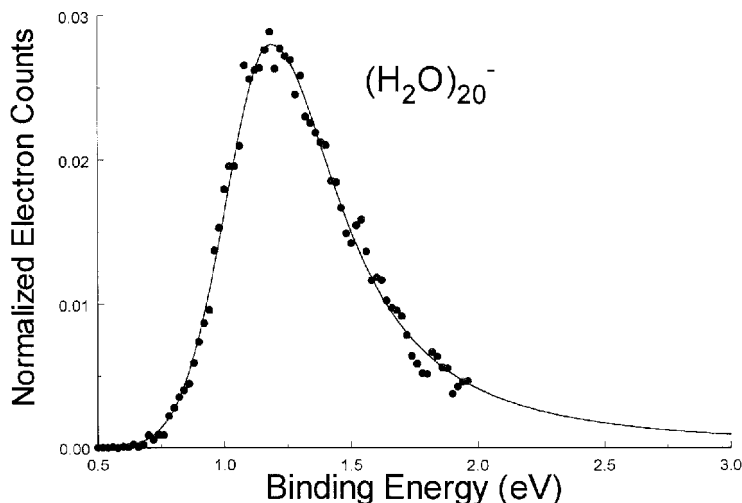


Figure 6. Fit of the $(\text{H}_2\text{O})_{20}^-$ photoelectron spectrum obtained by the Bowen group to the same empirical form that fits the hydrated electron's bulk absorption spectrum, namely a Gaussian to the low-binding-energy side of the spectral maximum and a Lorentzian form to the high-binding-energy side as in equation (7).

the Lorentzian width parameter characterizing the high-energy side and A is the shared amplitude of each section. An example of the fit is given in figure 6 which shows the photoelectron spectrum of $(\text{H}_2\text{O})_{20}^-$. The fit is excellent, with residuals revealing no systematic deviations.

Both the photoelectron data at $n = 11$ –28, 30, 34, 37, 47, 57 and 69 and the absorption data at $n = 11, 15, 20, 25, 30, 35, 40$ and 50 have been fitted to the form of equation (7). The fit parameters (peak centres E_{max} , Gaussian widths σ_G and Lorentzian widths σ_L) are plotted versus $n^{-1/3}$ in figure 7 including data from the bulk absorption spectrum of the hydrated electron. The peak centres of the photoelectron spectra (vertical detachment energies (VDEs)) proceed smoothly to bulk and have been fitted linearly in $n^{-1/3}$, giving

$$E_{\text{max, PES}}(n) = \text{VDE}_n = (-5.62 \pm 0.14 \text{ eV})n^{-1/3} + (3.248 \pm 0.049 \text{ eV}), \quad (8)$$

where the parameter uncertainties are estimated standard deviations and the standard deviation in VDE_n is 0.035 eV. The slope of -5.62 eV is very close to the continuum value based on the static and optical dielectric constants of water which varies from 5.56 to 5.9 eV with temperature. A value of 5.73 eV was reported (Coe *et al.* 1990) using fits to asymmetric Gaussians. The peak centres of the absorption spectra have also been fitted linearly in $n^{-1/3}$, giving

$$E_{\text{max, abs}}(n) = (-2.403 \pm 0.058 \text{ eV})n^{-1/3} + (1.783 \pm 0.019 \text{ eV}), \quad (9)$$

where the standard deviation in $E_{\text{max, abs}}$ is 0.021 eV. These data overlap with the photoelectron data at $n = 11$ and smoothly separate from the photoelectron data proceeding to the well-known maximum in the bulk absorption spectrum of $e^-(\text{aq})$ (Jortner 1971). The smooth progression in the absorption peak centres to a known bulk value and the smooth progression of the photoelectron data with the continuum law limiting slope gives confidence that the VDEs are progressing smoothly to a meaningful bulk intercept, $\text{VDE}_\infty = 3.25 \pm 0.05$ eV, which is a unique measurement

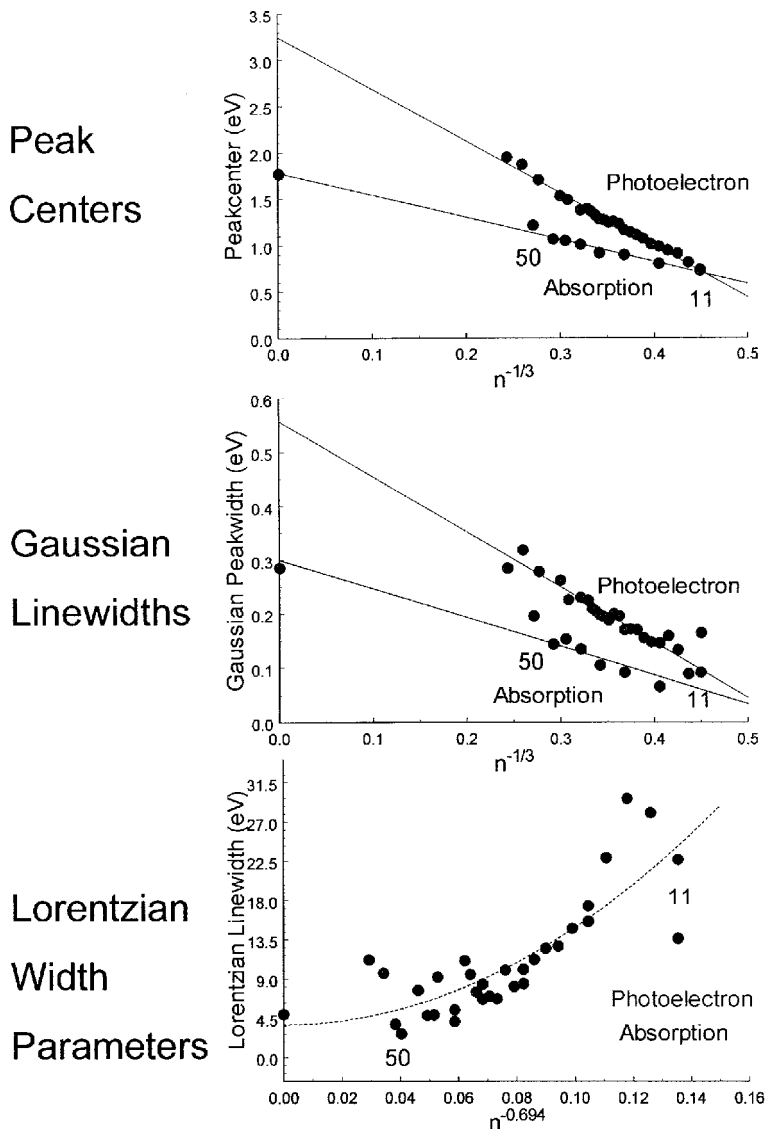


Figure 7. Plot of the three spectral shape fit parameters of equation (7) versus cluster size for the photoelectron data of the Bowen group and the absorption data of the Johnson group. Surprisingly, both the photoelectron data and the absorption data can be fit to the same form.

with no known bulk counterpart. The most probable reorganization energy for solvating water molecules about the electron of 1.6 eV (Coe *et al.* 1997) can be determined by subtracting the electron's hydration enthalpy (Jortner and Noyes 1966) from VDE_{∞} . The Gaussian widths of the low-energy sides of the spectra give similar results. The photoelectron and absorption data were fitted linearly in $n^{-1/3}$, giving

$$\sigma_{G, \text{PES}}(n) = (-1.025 \pm 0.050 \text{ eV}) n^{-1/3} + (0.557 \pm 0.018 \text{ eV}), \quad (10)$$

$$\sigma_{G, \text{abs}}(n) = (-0.533 \pm 0.034 \text{ eV}) n^{-1/3} + (0.300 \pm 0.011 \text{ eV}), \quad (11)$$

where the standard deviations in the widths are 0.013 and 0.011 eV respectively.

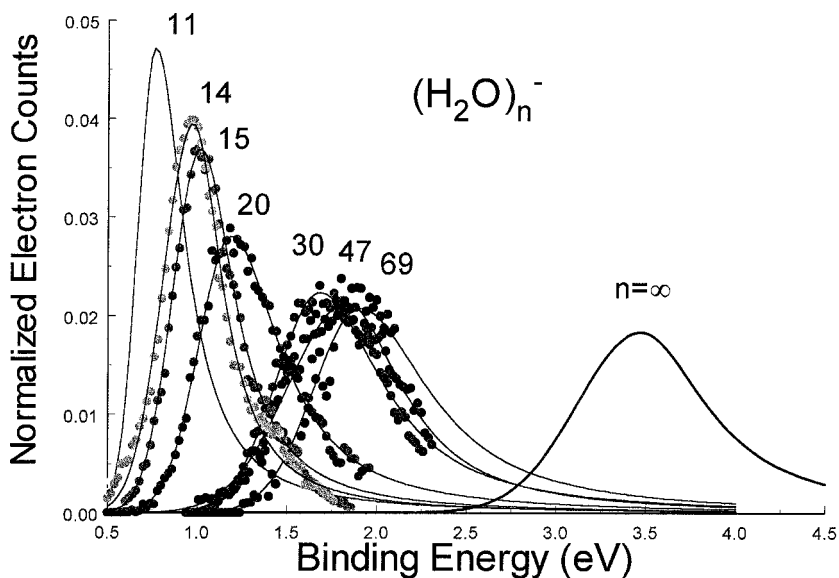


Figure 8. Normalized photoelectron spectra showing the smooth progression of the whole line-shape towards a bulk profile obtained by extrapolating the trends. This figure bears a striking resemblance to that given by Ayotte and Johnson (1997).

Again, the smooth progression of the absorption data to a known bulk value gives confidence that the photoelectron data are progressing smoothly to a meaningful bulk value.

The Lorentzian widths, characterizing the high-energy side of the spectra and the dynamics at work, fall essentially on the same plot. Whereas the peak centres and Gaussian widths separate smoothly and linearly in $n^{-1/3}$ from the $n = 11$ point, the photoelectron and absorption spectra share a common Lorentzian width at any given cluster size! The Lorentzian width data are not linear in $n^{-1/3}$ and have been fitted to the following purely empirical form:

$$\sigma_{L, \text{PES/abs}}(n) = (-6.90 \pm 1.1 \text{ eV})n^{-4/3} + (0.451 \pm 0.021 \text{ eV}), \quad (12)$$

with a standard deviation in width of 0.064 eV. Equations (8)–(12) enable the reproduction of the photoelectron and absorption spectra of any $(\text{H}_2\text{O})_n^-$ clusters at any size greater than $n = 11$, including the photoelectron spectrum at bulk.

3.2. Extrapolation of full photoelectron spectrum to the bulk

Fitting to the Gaussian–Lorentzian form of equation (7) has the additional advantage of enabling normalization of the spectra. The normalized photoelectron spectra are plotted in figure 8 which bears a striking resemblance to the plot of cluster absorption spectra shown by Ayotte and Johnson (1997). The photoelectron and absorption spectra of $(\text{H}_2\text{O})_{11}^-$ are almost identical even though the quantum-mechanical expressions for photoelectron and absorption spectroscopy are different (photons fixed versus tuned). One cannot help but wonder whether this similarity has something to do with the fact that $n = 11$ begins the continuous distribution in the mass spectrum of hydrated electron clusters (Haberland *et al.* 1984). We have used the

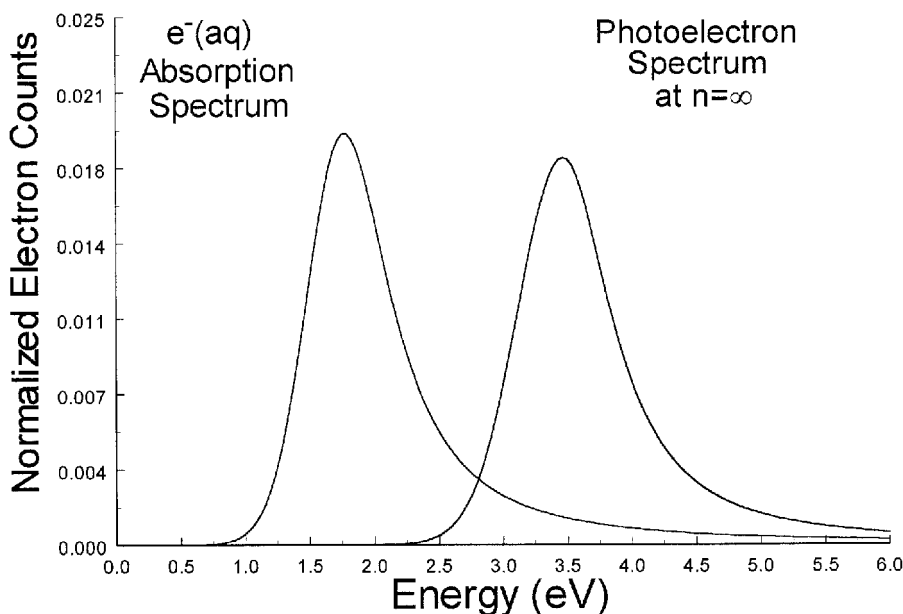


Figure 9. The bulk photoelectron spectrum plotted with an overlay of the bulk absorption spectrum. A significant range of the absorption spectrum's Lorentzian tail exists where there is almost no access to the conduction band as indicated by the low-binding-energy side of the photoelectron spectrum.

fit equations (8), (10) and (12) to determine the whole photoelectron spectrum at bulk (as plotted in figure 8) in contrast with previous work which only dealt with the peak centres (Coe *et al.* 1990). The bulk photoelectron and absorption spectra of the hydrated electron are given in figure 9 for comparison. Note that there is a fairly large gap between the maxima of these two bulk spectra. The photoelectron spectrum dies away in the region of the Lorentzian tail of the absorption spectrum. The absorption spectrum maintains a Lorentzian profile even in a region where there is almost no access to the conduction band. This suggests that the upper state in the absorption process of $e^-(aq)$ is not embedded in the conduction band, even though the upper state may lie above the adiabatic bottom of the conduction band. The upper state must be communicating readily with the conduction band to produce the Lorentzian tails, perhaps by means of solvent fluctuations. This idea will be folded into a new energy diagram of bulk water to be discussed after several other consequences of these results are discussed.

3.3. Surface versus internal issue in hydrated electron clusters

It is possible to make an internal or surface state of an excess electron when adding an electron to an $(H_2O)_n$ cluster (Barnett *et al.* 1988). Since $e^-(aq)$ is inherently an internal state, $(H_2O)_n^-$ properties must be internal (or perhaps internalizing) in order to extrapolate meaningfully to bulk as a constraint on the properties of $e^-(aq)$. Barnett *et al.* (1988) performed molecular dynamics calculations on $(H_2O)_n^-$ and found surface states of the excess electron to be more stable (adiabatically) at cluster sizes equal to or below $n = 32$. Internal states, analogous to $e^-(aq)$, were more stable at $n = 64$ and 128. VDEs were calculated for the internal states that were roughly twice those of the

surface states. The investigators suggested a transition from surface to internal excess electron states between $n = 32$ and $n = 64$ that would be evident in VDE measurements. Coe *et al.* (1990) reported measurements of the VDEs in the range $n = 11$ – 69 and found a smooth progression, linear in $n^{-1/3}$, with a slope close to the continuum value based on the static and optical dielectric constants of water (see equation (8)). The measured VDEs showed no transitions (nor does the absorption–dissociation data of the Johnson group) and were in accord with the calculated VDEs for surface states. The ‘bulk-like’ or ‘internal-like’ trend ($n^{-1/3}$ slope) in the experimental VDEs was apparently at odds with their agreement with the calculated surface state VDEs. The Bowen group suggested that the surface to internal transition was happening at $n \approx 11$ (smaller than predicted by theory), while others (Posey and Johnson 1988, Barnett *et al.* 1990) suggested that the transition was occurring at $n > 69$ (larger than predicted by theory). The situation was aptly described by Ayotte and Johnson (1997): ‘Thus, the deceptively complicated $(\text{H}_2\text{O})_n^-$ system has not yet yielded to self-consistent explanation of the experimental observations.’

The observation of a continuum trend in the VDEs alone was not convincing to proponents of the surface interpretation for $n = 11$ – 69 as there are ways that ‘more strongly bound’ surface states could give rise to internal-like trends (Cheshnovsky *et al.* 1995). In a good accounting of this state of affairs, Barnett *et al.* (1990) noted that the calculated internal VDEs extrapolate to a bulk value of 5.1 eV, which was considerably larger than the experimental extrapolation. They said: ‘This issue deserves further study on both the experimental and the theoretical side.’ One can make estimates of VDE_∞ , but this is basically an unknown quantity (until this issue is settled). A more important observation concerns the 9.8 eV $n^{-1/3}$ slope of the calculated VDEs which is almost twice the continuum value (5.6–5.9 eV) based on the static and optical dielectric constants of water. Over extended regions of $n^{-1/3}$ space, the continuum limit also constitutes a maximum for the trend. The internal state VDEs are overestimated by a factor of roughly two; so one is left to speculate on how much the surface state VDEs are overestimated. Agreement of the calculated surface states with the experimental data then is fortuitous and dielectrically calibrated surface state calculations are not likely to be in accord with the experimental data.

The primary motivation for plotting the photoelectron data of the Bowen group together with the absorption data of the Johnson group (as in figure 7) is that they reinforce each other with regard to connecting to bulk. The absorption data progress smoothly and linearly in $n^{-1/3}$ to a well known bulk value, while the photoelectron data progress smoothly and linearly in $n^{-1/3}$ towards an unknown bulk value, but with the continuum law slope determined by the static and optical dielectric constant of bulk water. This suggests that there will be no transitions at larger cluster sizes, in a way that cannot be argued from the photodetachment data alone. Perhaps more convincing is the unusual spectral shape (equation (7)) of both the cluster absorption and the photoelectron spectra, which is also shared by the bulk absorption spectrum of $e^-(\text{aq})$. The bulk spectral shape with the asymmetric tailing to the blue is no doubt a signature of the energetics and dynamics of $e^-(\text{aq})$. Seeing it in the cluster data argues that the clusters possess structural similarities that give rise to these features. Together, the experimental observations (the smooth progression of the absorption data to a known bulk value (Ayotte and Johnson 1997), the bulk slope of the VDE data, and the shared spectral profile of absorption and detachment cluster data with the bulk hydrated electron absorption spectrum) make a convincing case for the meaningful extrapolation of the cluster data to bulk for $e^-(\text{aq})$ properties.

3.4. *Threshold issues in water*

Threshold laws and their corresponding extrapolation schemes arise from the changes in the density of states associated with photoaccess within or outside a band of states. Thresholds can be obscured by the thermal population of initial states and the exponentially decaying density of final trapping states associated with band edges. Threshold laws allow the identification of band edges in spite of these effects and are valid as long as one is actually tuning the photon energy through a band edge. Water is more complicated regarding thresholds because water molecules dramatically reorganize themselves about charge. If initial and final states in a photo-initiated process involve different charges, then the product may require a significant difference in the arrangement of waters, which might be accomplished very slowly compared with the initiating photoevent (vertical process). As a result, vertical processes in water may run out of solvent overlap between the initial and final states even though the photons are of sufficiently high energy to access the lowest-energy states of the product. Such behaviour produces exponential spectral tails in threshold regions and is widespread in photophysical ionizing processes in water.

The low-energy sides of the photoelectron and absorption spectra are fitted quite rigorously by Gaussians which do not have thresholds. The data fall off exponentially, suggesting that they are governed by loss of solvent orientational overlap between a negatively charged reactant and a product that is either charge delocalized or uncharged. While it might be very interesting to search for deviations from the Gaussian form in the threshold regions of the photoelectron spectra, none is evident at the current signal-to-noise ratios. Experimental photoemission or photoionization thresholds in water do not indicate band edges for adiabatic states and must be regarded with great caution as constraints for locating adiabatic levels. They are often based on threshold laws assuming access to band edges which solvent overlap excludes. Such observations are very useful, however, as they actually map the shape of the potential energy of product states as a function of solvent reorganization about charge. In view of these considerations, it is particularly important to specify the manner in which a threshold is identified, and one might use words such as ‘apparent’ or ‘quasi’ to distinguish them from thresholds with vertical photoaccess to the band edge.

3.5. V_0 or the liquid electron affinity of water

The quantity V_0 (which is sometimes called the condensed-phase electron affinity) is the energy to promote a delocalized conducting electron of minimal energy into vacuum with zero kinetic energy. It indicates the bottom of the conduction band relative to the vacuum level. A good discussion of V_0 has been given by Han and Bartels (1990). Jortner’s (1971) considerations found that $-0.5 \text{ eV} < V_0 < 1.0 \text{ eV}$. Henglein (1974, 1977), who performed calculations on systems where solvent reorganization was important, found a value of -0.2 eV . It is now apparent to us that V_0 is much smaller in magnitude than accepted experimental values, such as the value of $-1.2 \pm 0.1 \text{ eV}$ given by Grand *et al.* (1979) and other experimental methods (Ballard 1972, Sass and Gerischer 1978). These results may require reinterpretation because they are often obtained with non-polar solvation models ($I_{\text{sol}} = I_{\text{gas}} + P_+ + V_0$) which cannot account fully for solvent reorganization, only the electronic polarization. It is also possible that the large magnitudes of these traditional V_0 values come from compensation for the use of the large ‘optical’ bandgap associated with pure water when the bandgap actually changes dramatically as a function of solvent re-

Table 3. The V_0 values and electron mobilities of various solvents (Holroyd and Allen 1971).

Solvent	V_0 (eV)	e^- mobility ($\text{cm}^2 \text{V}^{-1} \text{s}^{-1}$)
Water	?	0.002
n-hexane	+0.04	0.09
n-pentane	-0.01	0.16
Cyclopentane	-0.28	1.1
2,2,4-trimethylpentane	-0.18	7
Neopentane	-0.43	55
Tetramethylsilane	-0.62	90

organization (Coe *et al.* 1997) when ions are involved (as will be seen in the following sections).

Three arguments are offered in favour of a small V_0 value in water.

- (i) The most compelling evidence comes from the similarity of the ‘quasi’ threshold in the bulk photoelectron spectra (about 2.3 eV) and Kevan’s (1972) observed photoconductivity ‘quasi’ threshold (PCT) of hydrated electrons in ice (2.3 eV). If one picks an empirical law, such as extrapolation to the baseline of a tangent at the inflection point of the photoelectron peak, these ‘quasi’ thresholds extrapolate to a bulk value of about 2.3 eV. Now, in view of the revelations of the preceding section, we should attempt to be more explicit about these thresholds. Kevan’s 2.3 eV threshold corresponds roughly to a photobleaching efficiency of about 7% of its maximum value and about 2% efficiency at 2.1 eV. The bulk photoelectron spectra reaches 7% of its maximum intensity at 2.0 eV and 2% at 1.7 eV. These onsets track each other to the extent that ‘quasi’ thresholds can be trusted. In no way is the photoemission threshold 1.2 eV higher in energy as suggested by traditional V_0 values. These results suggest that V_0 is about 0.0 eV or perhaps even slightly positive.
- (ii) Holroyd and Allen (1971) have measured V_0 for a number of solvents and noted a relationship to the electron mobility. The V_0 values and electron mobilities for various solvents are presented in table 3 together with the electron mobility of water. The Holroyd–Allen relationship suggests that the V_0 value of water should be about zero or perhaps even slightly positive.
- (iii) Hoffman (Coe *et al.* 1997) has argued that V_0 might also be expected to be more negative with greater solvent polarizability. Since water can localize an electron in less than a picosecond (Migus *et al.* 1987), one might argue that only the optical polarizability should be considered for the delocalized electron property of V_0 in water. The optical polarizability of water ($3.70 \text{ cm}^3 \text{ mol}^{-1}$) is slightly smaller than the static polarizabilities of cryogenic methane ($6.7 \text{ cm}^3 \text{ mol}^{-1}$) and cryogenic argon ($4.06 \text{ cm}^3 \text{ mol}^{-1}$) for which orientation is not an issue. Reported V_0 values of liquid methane are -0.18 and -0.25 eV. The value for liquid argon is -0.21 eV. So these values suggest a small and perhaps slightly negative value for V_0 in water. It is concluded that the V_0 value in water is close to zero ($-0.2 \text{ eV} < V_0 < 0.3 \text{ eV}$) and significantly different from the traditional values in the literature.

3.6. *The anion problem and the adiabatic bandgap of water*

It has been a common practice in the literature to place the vacuum level relative to $\text{H}_2\text{O}(\text{l})$ using the photoemission threshold (PET) of water (Goulet *et al.* 1990). The bottom of the conduction band is then placed relative to the vacuum level by the value of V_0 . Using typical literature values, the PET is 10.06 eV (Delahay and Von Burg 1981) and $V_0 = -1.2$ eV (Grand *et al.* 1979), this approach defines a bandgap of 8.9 eV, which is grossly different from the adiabatic value of 7.0 eV presented herein. This common practice actually defines an ‘optical’ or ‘vertical’ bandgap that is specific to the initial state of pure water as accessible by the range of solvent fluctuations in $\text{H}_2\text{O}(\text{l})$. This ‘optical’ bandgap definition creates great difficulties when one tries to locate anions on a semiconductor diagram of water.

The following problems (collectively ‘the anion problem’) arise from using the ‘optical’ bandgap as the ‘adiabatic’ bandgap.

- (i) Given that $\text{OH}^-(\text{aq})$ is located 0.58 eV above $\text{H}_2\text{O}(\text{l})$ by virtue of the temperature dependence of K_w (Coe *et al.* 1997), the observed PET for $\text{OH}^-(\text{aq})$ of 8.45 eV (Delahay 1982) only reaches 9.03 eV above $\text{H}_2\text{O}(\text{l})$, which is not enough to reach the vacuum level based on 10 eV PET of water.
- (ii) By a thermochemical cycle described by Coe *et al.* (1997), the $\text{F}^-(\text{aq})$ defect state could be located about 8.1 eV below the vacuum level based on the 10 eV PET of water. This places $\text{F}^-(\text{aq})$ within the bandgap, suggesting that $\text{F}^-(\text{aq})$ will have a PET smaller than that of pure water. In fact it is easier to knock electrons off of $\text{H}_2\text{O}(\text{l})$ than $\text{F}^-(\text{aq})$ and no experimental PET for $\text{F}^-(\text{aq})$ exists (Delahay 1982). This suggests that $\text{F}^-(\text{aq})$ lies below $\text{H}_2\text{O}(\text{l})$ and not within the bandgap.
- (iii) If $\text{e}^-(\text{aq})$ were placed 1.7 eV (Jortner and Noyes 1966) (solvation enthalpy) below the vacuum level based on the 10 eV PET of water, then it would require 8.3 eV photons to produce hydrated electrons from pure water. In fact, the spectrum of $\text{e}^-(\text{aq})$ is observed with as little as 6.5 eV photons (Han and Bartels 1990).
- (iv) If we use thermochemical cycles to locate the anionic defect states (Coe *et al.* 1997) of $\text{e}^-(\text{aq})$, $\text{I}^-(\text{aq})$, $\text{Br}^-(\text{aq})$, $\text{OH}^-(\text{aq})$ and $\text{Cl}^-(\text{aq})$ and then plot the literature photoemission thresholds for each anion (as shown in figure 10), we find that none of them reaches the vacuum level based on the 10 eV PET of water.

Given, the ‘anion problem’, it is clear that an ‘adiabatic’ vacuum level and bandgap must be defined and carefully distinguished from the common use of bandgap which generally (in the context of pure water) might be denoted the ‘optical’ or ‘vertical’ bandgap of pure water. Clearly the ‘adiabatic’ vacuum level should lie below the PET arrowheads in figure 10, which access the lowest energy, that is that of $\text{e}^-(\text{aq})$. Likewise, the conduction band must extend down to about 7 eV even though this part of the conduction band is not accessible from solvent configurations of pure water or the solvent configurations associated with strongly solvated ions. Now, a 3 eV change in the positioning of the vacuum level is certainly dramatic, but most (about two thirds) of this difference is semantic in that it deals with being specific about the difference between ‘vertical’ and ‘adiabatic’ properties. About one third of the difference can be attributed to the cluster data, producing a diminished magnitude of V_0 . The PETs have been arranged in figure 10 to emphasize the fact that anions lying deeper into the bandgap have minimum access at higher energies. This observation is

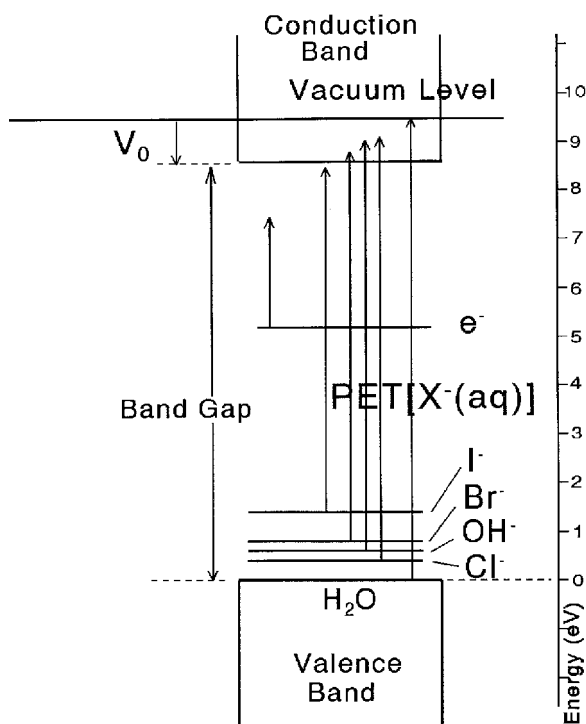


Figure 10. An amorphous semiconductor diagram of water where the vacuum level is defined by the PET of water and the V_0 value by traditional experimental values. Anionic defect states are located in the bandgap and literature PETs are plotted from each state (Coe *et al.* 1997). None of the anionic PETs reaches this vacuum level because it is actually a vertical property. The adiabatic vacuum level must lie below the PET arrowhead which accesses the lowest energy, that of $e^-(aq)$. It is important to distinguish the ‘optical’ vacuum level pictured here from the ‘adiabatic’ vacuum level needed to reconcile anion energetics and photophysics.

an additional clue, implicating solvent orientation about charge as the critical factor to be added to the picture.

3.7. The chemical identity and value of the adiabatic bandgap of water

To proceed any further, we must consider the chemical identity (Coe *et al.* 1997) of the lowest-energy states in the conduction band. Vertical photoionization of $H_2O(l)$ produces an internally excited H_2O^+ ion (in the geometry of the neutral) and a delocalized e^- . The H_2O^+ is unstable and attacks the nearby water, producing H_3O^+ and OH. The bottom of the conduction band is associated with complete relaxation of solvating water about the H_3O^+ and OH species, and the minimum kinetic energy of the delocalized electron, but not with solvent reorientation about the electron or it localizes, that is the conduction-band edge is $H_3O^+(aq) + OH(aq) + e^-(cond)$. With this definition, it is a straightforward matter to couple reactions of known energies to locate the adiabatic conduction-band edge 7.0 eV above $H_2O(l)$. The difference from the 6.9 eV result of Coe *et al.* (1997) is the current preference for $V_0 = 0.0$ eV rather than -0.1 eV. Since solvent molecules must significantly reorient about the H_3O^+ species, the conduction-band edge ($H_3O^+(aq) + OH(aq) + e^-(cond)$) is vertically

inaccessible from $\text{H}_2\text{O}(\text{l})$. Consequently, there can be no direct optical measurements of the adiabatic bandgap of water.

3.8. *New bulk energy diagram of water*

To reconcile anion energetics and the generic semiconductor diagram of figure 10, one must add a dimension for solvent orientation. All the above considerations concerning the adiabatic bandgap, the adiabatic vacuum level and the chemical identity of the conduction-band edge have been folded into an energy diagram for bulk water in figure 11 together with a schematic coordinate for reorientation of water about charge. This figure is taken largely from figure 5 of Coe *et al.* (1997) except that it has been folded in half to separate the effects of cation solvation from those of anion solvation. This is a small but significant change. The drawing starts by identifying the top of the valence band in figure 10 with $2\text{H}_2\text{O}(\text{l})$ in figure 11. We need two water molecules in order to maintain charge and atom balance for all states of interest, given that we have used two water molecules in the chemical identity of the conduction-band edge. Note that all the adiabatic states on the anion solvation side of the drawing carry along the $\text{H}_3\text{O}^+(\text{aq})$ species; so these states are distinguished by their anions and could be uniquely denoted by the anions.

To understand the diagram better, several depicted photophysical processes are described in more detail. The breadth of the lines representing adiabatic states is along the ion solvation coordinate and schematically represents the range of solvent fluctuations in this coordinate. A solvent fluctuation of $\text{H}_2\text{O}(\text{l})$ that points the negative end of a neighbouring water's dipole moment towards the target molecule (the one to be ionized), is one that moves inwards in the diagram along the cation solvation coordinate. The experimental PET of water is drawn from the inner edge of the $2\text{H}_2\text{O}(\text{l})$ state as these fluctuations are more like the final product. Since there are no solvent fluctuations of $\text{H}_2\text{O}(\text{l})$ that go all the way to the orientation of water about $\text{H}_3\text{O}^+(\text{aq})$, the PET of water cannot extend down to the adiabatic conduction-band edge. The PET indicates the point at which $\text{H}_2\text{O}(\text{l})$ fluctuations run out of overlap with the region of the conduction band associated with $\text{H}_2\text{O}^{+*} + \text{H}_2\text{O}(\text{l})$, rapidly becoming incompletely solvated, $\text{H}_3\text{O}^{+*} + \text{OH}$. The PET determines the shape of the conduction-band potential in this region and not the adiabatic location of any states. On time scales longer than the optical process, solvent reorganizes about the $\text{H}_3\text{O}^+ + \text{OH}$, conveying considerable stabilization. Complete relaxation places the conduction-band edge only 7.0 eV above $\text{H}_2\text{O}(\text{l})$. Given the small value of $V_0 \approx 0.0$ eV, the vacuum level tracks the conduction band very closely. Both are strong functions of the ion solvation coordinate.

Moving to the anions, consider the ionic dissociation of water. The production of a strongly solvated H_3O^+ moves the ionically dissociated state to the centre of the diagram (the bend in the diagram corresponds to optimal H_3O^+ solvation and no anion solvation). Solvation of OH^- takes the ionically dissociated state out to the far right edge of the diagram because OH^- is strongly solvated. Since H_3O^+ is commonly shared by all states on this side of the diagram, this state can also be labelled the OH^- anionic defect state. The PET of $\text{OH}^-(\text{aq})$ is placed on the inside of the state's line as these fluctuations are less strongly solvating and more like the neutral product of the detachment process. Like the PET of water, the PET of $\text{OH}^-(\text{aq})$ does not indicate the location of an adiabatic state; rather it fixes the location of the vacuum level relative to solvent orientation about OH^- . Again the vacuum level and conduction band are strong functions of ion solvation, and the thresholds serve to map the shape of the

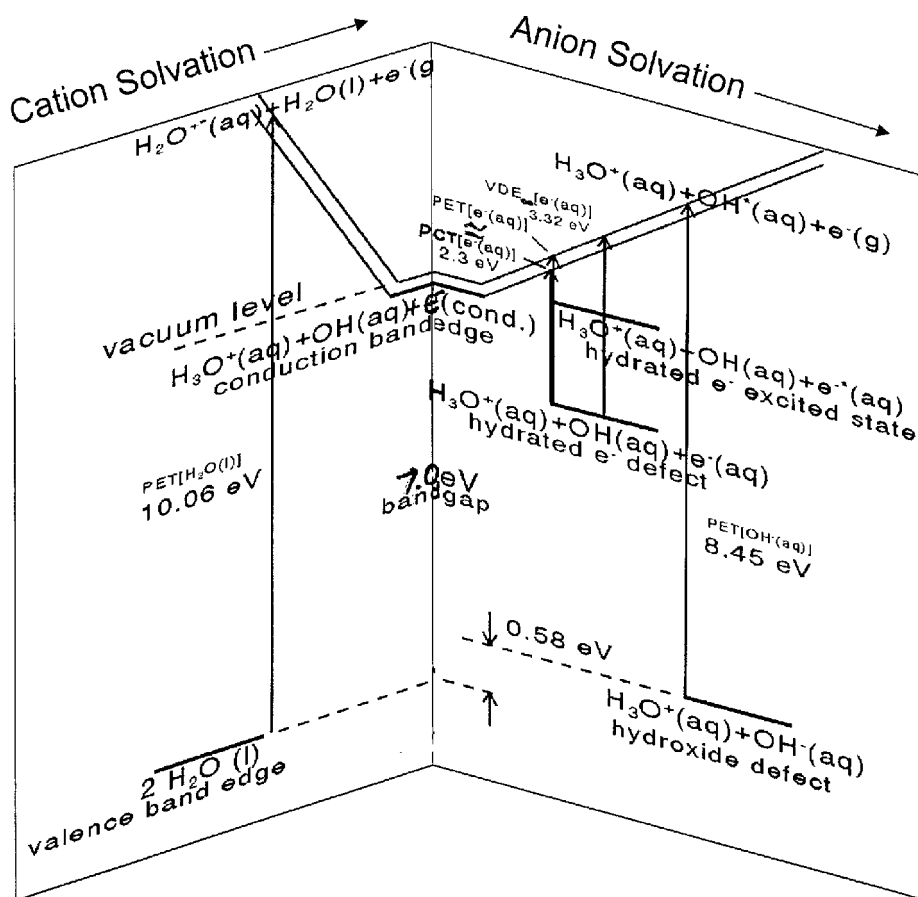


Figure 11. A new bulk energy diagram for water that schematically incorporates ion solvation into the generic amorphous semiconductor picture. This figure is essentially figure 5 from Coe *et al.* (1997) except that it has been folded in half to separate the effects of cation and anion solvation. Literature PETs map the shape of the conduction band as a function of solvent reorganization about charge, rather than identifying the adiabatic locations of states. The picture merges the energetics of solvated anions and pure water in a manner consistent with the observed photophysics of each.

conduction band and vacuum level as functions of solvent reorganization about charge.

If we start with the delocalized conducting electron at the minimum of the conduction band, it takes less than a picosecond to localize into the hydrated electron state (Migus *et al.* 1987). The $e^-(aq)$ anionic defect state ($H_3O^+(aq) + OH(aq) + e^-(aq)$) is located below the vacuum level minimum by 1.7 eV, the electron's solvation enthalpy (Jortner and Noyes 1966). Since $e^-(aq)$ is less strongly solvated than $OH^-(aq)$, it does not extend as far along the anion solvation coordinate. Note that the $e^-(aq)$ state is positioned 5.3 eV above $H_2O(l)$ which is not at odds with the 6.5 eV experimental thresholds for seeing $e^-(aq)$ from pure water (Han and Bartels 1990). The VDE obtained from extrapolating the peak centres of cluster photoelectron spectra to bulk is plotted from the centre of the $e^-(aq)$ state line because a vertical process accesses geometries in the upper state that are most like the initial state. The PET of

$e^-(aq)$, which is similar to the PCT of $e^-(ice)$, is shown from the less strongly solvating side of the state's line as with the other thresholds.

The way that the thresholds map the shape of the vacuum level and conduction band has interesting consequences for the set of electronically excited p-states of $e^-(aq)$. As these states are more diffuse, they will no doubt be less strongly solvated than the ground s-state of $e^-(aq)$. Making use of the conclusions drawn from the comparison of the bulk absorption and photoelectron spectra (figure 9), we must configure our energy diagram such that the minimum energies of the p-states of $e^-(aq)$ are not embedded in the conduction band, even though these states may lie above the adiabatic bottom of the conduction band. The conduction band rises with increased anion solvation, leaving a space for the p-states to exist even though they have energies similar to the conduction-band minimum. While there are likely to be some less stable solvent configurations of the p-states embedded in the conduction band, it is interesting that the most stable configurations of the p-states are connected to the conduction band by the anion solvation coordinate, that is by solvent fluctuations. These considerations are no doubt important in explaining the Lorentzian tail in the absorption spectrum of the hydrated electron.

This new energy diagram assimilates a range of photophysical observations from both pure water and anions in water. It provides a consistent framework for understanding both types of data. When one looks at just the right-hand side of figure 11 (the side of interest for the study of anions in water), it is striking how different this picture is from the left-hand side (the side of interest for the study of pure water). Hopefully this new picture will prove useful in formulating new ideas. The next step will be to quantify the ion solvation coordinates, hopefully in one dimension, perhaps based on the reorganization energies associated with various solvent configurations.

4. Conclusions

The successful connection of cluster ion quantities to bulk has led to major reassessments of a number of fundamental properties associated with water. The development of the cluster-pair-based common-point method has enabled an independent determination of the proton's absolute hydration enthalpy and free energy from ion clustering data without extrathermodynamic assumptions. The value of -1151.0 ± 2.2 kJ mol⁻¹ for the proton's absolute hydration enthalpy falls slightly outside the traditional range of results. The cluster-pair-based common-point method determines a value of -1103.2 ± 1.1 kJ mol⁻¹ for the proton's absolute hydration free energy. This result seems to fall towards the negative side of the traditional range; so it is not really as controversial as the enthalpy result, and there are recent computational investigations supporting it (Tawa *et al.* 1998). The method is now sufficiently well understood that it can be used to estimate the bulk hydration values of ions without bulk data on corresponding salts. It also seems applicable to other solvents, such as ammonia, where in general much less is known than in water.

The extrapolation of hydrated electron results to bulk has given rise to new evaluations of the V_0 and bandgap of water. The combined consideration of the photoelectron and absorption cluster data sets strengthens the case for meaningful extrapolation to bulk. The spectral signature of the bulk hydrated electron absorption spectra is shared with both the photoelectron and the absorption cluster spectra reinforcing the connection to bulk. A set of five equations have been presented which allow the generation of the spectral shape of either the absorption or the photoelectron data at any cluster size greater than or equal to 11, with only ten parameters. The

extrapolation of the whole photoelectron spectrum to bulk allows a more in-depth examination of the issue of thresholds in water. The similarity of the onset of the bulk photoelectron spectrum with the photoconductivity onset of hydrated electrons in ice (Kevan 1972) presents the strongest argument to date that $V_0 \approx 0.0$ eV in water and much smaller than traditional values. The desire to place solvated anions, such as $e^-(aq)$ and $OH^-(aq)$, on to the energy diagram of bulk water, has led to the definition of an adiabatic bandgap of water ($H_3O^+(aq) + OH^-(aq) + e^-(cond)$) which is located 7.0 eV above $H_2O(l)$. This may be contrasted with traditional definitions of the bandgap (usually in the vicinity of 8.7 eV) which are actually ‘optical’ or ‘vertical’ bandgaps associated with solvent configurations of pure water and determined with large negative V_0 values which appear to be in error. A new energy diagram is presented for bulk water that schematically incorporates the effect of solvent reorientation about charge into the amorphous semiconductor picture. This picture illustrates how literature PETs map the shape of the conduction band as a function of anion or cation solvation coordinates, rather than identifying adiabatic locations of states. The picture merges the energetics of solvated anions and pure water in a manner consistent with the observed photophysics of each.

Work is currently being pursued on connecting the properties of neutral water clusters to bulk ice. It will be interesting to see whether equally fundamental reassessments lie in store upon the successful connection to bulk.

References

- ATKINS, P. W., 1994, *Physical Chemistry* (New York: W. H. Freeman).
- AYOTTE, P., and JOHNSON, M. A., 1997, *J. chem. Phys.*, **106**, 811.
- BALLARD, R. E., 1972, *Chem. Phys. Lett.*, **16**, 300.
- BARNETT, R. N., LANDMAN, U., CLEVELAND, C. L., and JORTNER, J., 1988, *J. chem. Phys.*, **88**, 4429.
- BENTLEY, J., COLLINS, J. Y., and CHIPMAN, D. M., 2000, *J. phys. Chem. A*, **104**, 4629.
- CAMPAGNOLA, P. J., LAVRICH, D. J., DELUCA, M. J., and JOHNSON, M. A., 1991, *J. chem. Phys.*, **94**, 5240.
- CHESHNOVSKY, O., GINIGER, R., MARKOVICH, G., MAKOV, G., NITZAN, A., and JORTNER, J., 1995, *J. Chim. phys. Phys.-Chim. biol.*, **92**, 397.
- COE, J. V., 1986, PhD Thesis, The Johns Hopkins University; 1994, *Chem. Phys. Lett.*, **229**, 161; 1997, *J. phys. Chem. A*, **101**, 2055.
- COE, J. V., BOWEN, K. H., and JOHNSON, M. A., 2001 (to be published).
- COE, J. V., EARHART, A. D., COHEN, M. H., HOFFMAN, G. J., SARKAS, H. W., and BOWEN, K. H., 1997, *J. chem. Phys.*, **107**, 6023.
- COE, J. V., LEE, G. H., EATON, J. G., ARNOLD, S. T., SARKAS, H. W., BOWEN, K. H., LUDEWIGT, C., HABERLAND, H., and WORSNOP, D. R., 1990, *J. chem. Phys.*, **92**, 3980.
- COHEN, M. H., SCHWOPE, T., TISSANDIER, M., and COE, J. V., 1996, *Proceedings of the Third Workshop on Dissociative Recombination* (Singapore: World Scientific), pp. 216–225.
- DELAHAY, P., 1982, *Accts chem. Res.*, **15**, 40.
- DELAHAY, P., and VON BURG, K., 1981, *Chem. Phys. Lett.*, **83**, 250.
- FELLERS, D., GLENDENING, E. D., WOON, D., and FEYEREISEN, M. W., 1995, *J. chem. Phys.*, **103**, 3526.
- FRIEDMAN, H. L., and KRISHNAN, C. V., 1973, *Thermodynamics of Ionic Hydration, Water: A Comprehensive Treatise*, vol. 3, edited by F. Franks (New York: Plenum), pp. 1–118.
- FRISCH, M. J., TRUCKS, G. W., *et al.*, 1995, Gaussian 94 (Pittsburgh, Pennsylvania: Gaussian, Inc.).
- GOLDEN, S., and TUTTLE, J. T. R., 1981, *J. chem. Soc., Faraday Trans. II*, **77**, 889.
- GOULET, T., BERNAS, A., FERRADINI, C., and JAY-GERIN, J. P., 1990, *Chem. Phys. Lett.*, **170**, 492.
- GRAND, D., BERNAS, A., and AMOUYAL, 1979, *Chem. Phys.*, **44**, 73.
- GRUNWALD, E., and STEEL, C., 1996, *Int. Rev. phys. Chem.*, **15**, 273.

- HABERLAND, H., LANGOSCH, H., SCHINDLER, H. G., and WORSNOP, D. R., 1984, *J. phys. Chem.*, **88**, 3903.
- HALLIWELL, H. F., and NYBURG, S. C., 1963, *Trans. Faraday Soc.*, **59**, 1126.
- HAN, P., and BARTELS, D. M., 1990, *J. phys. Chem.*, **94**, 5824.
- HENGLEIN, A., 1974, *Ber. Bunsenges. phys. Chem.*, **78**, 1078; 1977, *Can. J. Chem.*, **55**, 2112.
- HOLROYD, R. A., and ALLEN, M., 1971, *J. chem. Phys.*, **54**, 5014.
- JOLLY, W. L., 1952, *Chem. Rev.*, **50**, 351; 1954, *J. phys. Chem.*, **58**, 250.
- JORTNER, J., 1971, *Ber. Bunsenges. phys. Chem.*, **75**, 696.
- JORTNER, J., and NOYES, R. M., 1966, *J. phys. Chem.*, **70**, 770.
- KEBARLE, P., 1974, *Gas-Phase Ion Equilibria and Ion Solvation, Modern Aspects of Electrochemistry*, vol. 9, edited by B. E. Conway and J. O. M. Bockris (New York, Plenum), pp. 1–46.
- KEESEE, R. G., and CASTLEMAN, J. A. W., 1980, *Chem. Phys. Lett.*, **74**, 139; 1986, *J. phys. Chem. Ref. Data*, **15**, 1011.
- KEESEE, R. G., LEE, N., *et al.*, 1980, *J. chem. Phys.*, **73**, 2195.
- KEVAN, L., 1972, *J. phys. Chem.*, **76**, 3830.
- KLOTS, C. E., 1981, *J. phys. Chem.*, **85**, 3585.
- LEE, G. H., ARNOLD, S. T., EATON, J. G., SARKAS, H. W., BOWEN, K. H., LUDEWIGT, C., and HABERLAND, H., 1991, *Z. Phys. D*, **20**, 9.
- LEE, N., KEESEE, R. G., and CASTLEMAN, J. A. W., 1980, *J. Colloid Interface Sci.*, **75**, 555.
- LIAS, S., 1997, <http://webbook.nist.gov/chemistry/ion>.
- LINDE, D. R., 1997, *CRC Handbook of Chemistry and Physics* (Boca Raton, Florida: CRC Press).
- LU, D., 1996, PhD Thesis, The Ohio State University.
- LU, D., and SINGER, S. J., 1996, *J. chem. Phys.*, **105**, 3700.
- MALAXOS, S., TUTTLE, J. T. R., and COE, J. V., 2001 (to be published).
- MARCUS, Y., 1987, *J. chem. Soc., Faraday Trans. I*, **83**, 2985; 1994, *Biophys. Chem.*, **51**, 111.
- MARX, D., TUCKERMAN, M. E., HUTTER, J., and PARINELLO, M., 1999, *Nature*, **397**, 601.
- MIGUS, A., GAUDUEL, Y., MARTIN, J. L., and ANTONETTI, A., 1987, *Phys. Rev. Lett.*, **58**, 1559.
- PLASTRIDGE, B., COHEN, M. H., COWEN, K. A., WOOD, D. A., and COE, J. V., 1995, *J. phys. Chem.*, **99**, 118.
- POSEY, L. A., CAMPAGNOLA, P. J., JOHNSON, M. A., LEE, G. H., EATON, J. G., and BOWEN, K. H., 1989, *J. chem. Phys.*, **91**, 6536.
- POSEY, L. A., and JOHNSON, M. A., 1988, *J. chem. Phys.*, **89**, 4807.
- RANDLES, E. B., 1956, *Trans. Faraday Soc.*, **52**, 1573.
- SASS, J. K., and GERISCHER, H., 1978, *Interfacial Photoemission*, edited by Feuerbacher, B. Fitton and R. F. Willis (New York: Wiley), pp. 469–500.
- SCHINDEWOLF, U., 1982, *Ber. Bunsenges. phys. Chem.*, **86**, 887.
- SU, Y., and TRIPATHI, G. N. R., 1992, *Chem. Phys. Lett.*, **188**, 388.
- TAWA, G. J., TOPOL, I. A., BURT, S. K., CALDWELL, R. A., and RASHIN, A. A., 1998, *J. chem. Phys.*, **109**, 4852.
- TISSANDIER, M. D., COWEN, K. A., FENG, W. Y., GUNDLACH, E., COHEN, M. H., EARHART, A. D., COE, J. V., and TUTTLE, T. R., 1998, *J. phys. Chem. A*, **102**, 7787.
- TRASATTI, S., 1979, *Solvent Adsorption and Double-Layer Potential Drop at Electrodes, Modern Aspects of Electrochemistry*, vol. 13, edited by B. E. Conway and J. O'M. Bockris (New York: Plenum), pp. 81–206.
- TUTTLE, J. T. R., and GOLDEN, S., 1981, *J. chem. Soc., Faraday Trans. II*, **77**, 873.
- WEAST, R. C. (editor), 1985, *CRC Handbook of Chemistry and Physics* (Boca Raton, Florida: CRC Press).
- WEIS, P., KEMPER, P. R., BOWERS, M. T., and XANTHEAS, S. S., 1999, *J. Am. chem. Soc.*, **121**, 3531.
- XANTHEAS, S. S., 1996, *J. phys. Chem.*, **100**, 9703.
- XANTHEAS, S. S., and DANG, L. X., 1996, *J. phys. Chem.*, **100**, 3989.